Nematic Nanotube Gels

M. F. Islam, A. M. Alsayed, Z. Dogic, J. Zhang, T. C. Lubensky, and A. G. Yodh
Department of Physics and Astronomy, University of Pennsylvania, 209 S. 33rd Street, Philadelphia, Pennsylvania 19104-6396, USA
(Received 15 October 2003; published 27 February 2004)

We report the creation of nematic nanotube gels containing large domains of isolated, oriented, half-micron-long, single-wall carbon nanotubes (SWNTs). We make them by homogeneously dispersing surfactant coated SWNTs at low concentration in an *N*-isopropyl acrylamide gel and then inducing a volume-compression transition. These gels exhibit hallmark properties of a nematic: birefrigence, anisotropy in optical absorption, and disclination defects. We also investigate the isotropic-to-nematic transition of these gels, and we describe the physical properties of their ensuing nematic state, including a novel buckling of sample walls. Finally, we provide a simple model to explain our observations.

DOI: 10.1103/PhysRevLett.92.088303 PACS numbers: 82.70.Gg, 64.70.Md, 81.05.Qk, 81.07.Bc

Isolated single-wall carbon nanotubes (SWNTs) possess truly remarkable mechanical, electrical, optical, and thermal properties [1–4]. Many of their anticipated materials applications require macroscopically aligned samples of SWNTs [3–8]. With few exceptions [6–8], solutions and solid-phase mixtures of SWNTs produced thus far have been isotropic. Apparently, the dispersal of SWNTs at sufficient concentration to create nematic phases is inhibited by the strong van der Waals attraction between nanotubes that favors aggregation. By coating our nanotubes with sodium dodecyl benzene sulfonate surfactant (NaDDBS) [9], we have been able to reduce the effect of attractive interactions and achieve relatively high concentrations of isolated SWNTs in water. Nevertheless, we have not observed nematic order in suspensions with nanotube concentrations as high as 10 mg/ml, in clear violation of Onsager theory for hard rods [10] which predicts an isotropic-nematic (I-N) transition at critical concentrations of order 1.1 mg/ml [11]. Evidently strong attractive interactions remain important, creating multitube bundles with larger effective diameters, or more complex tube networks in suspension.

In this Letter we report on heretofore unachieved concentration and degree of alignment of isolated SWNTs by first dispersing SWNTs at low concentration (1.34 mg/ml [12]) in an aqueous solution of isopropyl acrylamide monomer that is then polymerized and cross-linked to form a gel [13]. Then the solvent quality of the gel is reduced by increasing temperature, and the composite system undergoes a phase transition with a large compressional volume change. After volume compression, SWNTs in the more concentrated samples align locally, while their concentration (c_{SWNT}) remains spatially homogeneous. We conclude from these observations that the gel plays at least two important roles: it prevents the close contact between parallel nanotubes that produces bundling, and it compresses the nanotubes to produce concentrations of isolated nanotubes, not accessible in simple aqueous suspensions, that favor their alignment.

Our nanotubes were obtained in raw form from Tubes@Rice (laser-oven SWNTs, batch P081600) and purified according to the procedure described in Ref. [14]. The purified laser-oven nanotubes were >90 wt% SWNTs. We dispersed these tubes in water using NaDDBS surfactant ($C_{12}H_{25}C_6H_4SO_3Na$) [9]. The resultant nanotube dispersions were ~90 5% single tubes with average length $L \sim 516$ 286 nm [9] at a concentration of 0.1 mg/ml. They were stable in suspension for concentrations up to ~10 mg/ml, albeit as a mixture of isolated and small bundles of SWNTs.

The gel consisted of polymerized *N*-isopropyl acrylamide polymer (NIPA; 492 mM), *N, N′*-methylenebisacrylamide (cross-linker agent; 1.8 mM), ammonium persulfate (initiator; 1.88 mM), and *N, N, N′, N′*-tetramethylethylenediamine (accelerator at 295 K; 25 mM). Vortexed SWNT-NIPA pregel solutions were loaded into rectangular capillary tubes and then concurrently polymerized and cross-linked at 295 K in ~3 h. For polymerization at 295 K the gel network and tube distribution is fairly homogeneous. After gelation, the nanotubes weakly associate to the gel network but do not form chemical bonds. Their orientation and center of mass were randomly distributed to form a dilute macroscopically homogeneous and isotropic dispersion within the gel. The resultant gel mixtures were immersed inside glass vials containing 20 mM Trizma buffer and placed in an oven at 323 K. At this temperature the polymer network in the gel became hydrophobic and the gel collapsed, expelling water in the process. We then removed the expelled water from the capillary and made microscopic observations on the shrunken SWNT-NIPA gels. Removal of expelled water prevented the gel from swelling back to its original volume when the temperature was lowered to 295 K during imaging. After imaging, the gels were again in 20 mM Trizma buffer at 323 K. *The gels do not dry out during imaging or when they are stored in the oven immersed in buffer; water remains in the collapsed gel.*

In Figs. 1(a) and 1(b) we show photographs of SWNT-NIPA gels before and after shrinking. After a volume compression of ~8 , the typical sample dimensions of the shrunken gels were ~2 cm 2 mm 0.1 mm. Gels appear darker after shrinking than before because the nanotube concentration is higher. Optical microscopy, capable of identifying SWNT aggregates of diameter 50 nm or larger, shows no evidence of SWNT aggregation in any sample before or after shrinking. Furthermore, position-dependent absorption measurements using unpolarized light did not detect any SWNT concentration inhomogeneity. Our samples exhibited striking macroscopic properties. As illustrated in Fig. 1(c), their surfaces can undulate and buckle upon compression. At very low concentrations (c_{SWNT} 2.47 mg/ml), the 2 cm 0.1 mm sidewalls, the 2 mm 0.1 mm end walls, and the 2 cm 2 mm top and bottom walls are flat. At concentrations above $c_{SWNT} \geq 3.30$ mg/ml, which we identify shortly as the critical concentration (c_{crit}) for the I-N transition in the bulk, the side walls first undulate and then develop cusplike modulations upon further volume decrease [see Fig. 1(d)]. The undulations of the two sidewalls are out of phase and produce a peristaltic distortion of the sample. In scanning electron microscope images, we also observed smooth in-phase undulations of the top and bottom walls corresponding to a sinusoidal bending of the whole sample. Sharp buckling of the top and bottom walls was not observed.

Images of sample birefringence enabled us to quantitatively characterize and map out nanotube alignment. We inserted our gels between crossed polarizers in a Leica inverted optical microscope and recorded images using a charge-coupled device camera (640 480 pixels) and an 8-bit video frame grabber. Isotropic regions and those with nanotubes aligned along one of the polarizer axes appear dark. Those regions with nanotubes aligned in the plane of the polarizers and oriented at 45 to their axes appear brightest. We derived semiquantitative information about the degree of nanotube alignment across a broad range of samples, by taking care to maintain the source intensity and the video gain/offset constant for the full set of images.

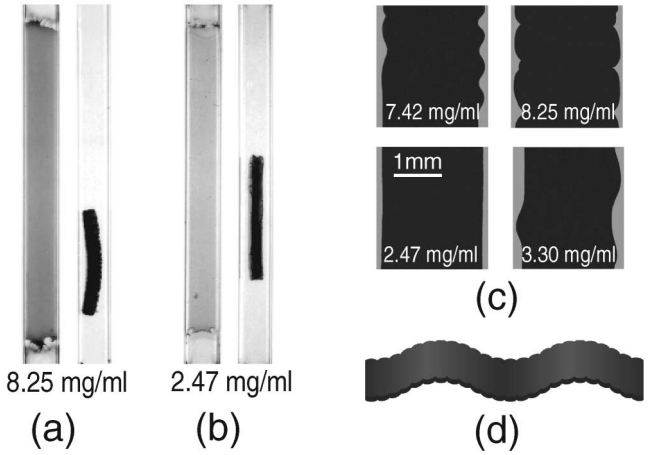

FIG. 1. (a),(b) Capillary tubes containing SWNT-NIPA gels before and after shrinking. NIPA gels prepared with surfactant only shrank by almost the same ratio. (c) The surfaces of the shrunken SWNT-NIPA gels can undulate and buckle upon compression. (d) A schematic representation of the nanotube gels with $c_{SWNT} \geq 3.30$ mg/ml.

The primary features of the time and concentration dependence of our observations are summarized in Fig. 2. Before shrinking, all samples were isotropic: cross-polarized light transmission through these samples was zero for all orientations. Birefringence was observed only in volume-compressed samples. Twenty minutes after shrinking, SWNT-NIPA gels with $c_{SWNT} \geq 8.25$ mg/ml exhibited birefringence. Thereafter, the samples slowly underwent further alignment. Alignment was always stronger at the sample edges than at its center. After four days, very little additional order was observed. For comparison we exhibit the time evolution of a dilute sample (0.82 mg/ml). Birefringence appeared near the sample edges after two days; subsequent evolution and stabilization of the birefringence was again achieved within four days. Clearly some nanotube alignment occurred in dilute samples (especially near the sample edges), but alignment took longer and was weak compared to concentrated samples. As a reversibility check we allowed the shrunken gels to expand to their original size (by adding water), and the reswollen gels were again isotropic.

In Fig. 3(a) we show a four-day-old sample (c_{SWNT} 8.25 mg/ml) with its long axis oriented at 0 and 45 with respect to one polarizer axis. The gel exhibited a maximum birefringence when its edges were oriented 45 with respect to the input polarizer pass axis, suggesting the sidewalls play a significant role in determining nanotube orientation. Tube alignment appears larger near the gel edges. The top surface in the sample rotated at 45 with respect to the polarizers shows alternating light and dark regions. When we rotate the sample out of the plane by ~30 about an axis coincident with its short edge, the

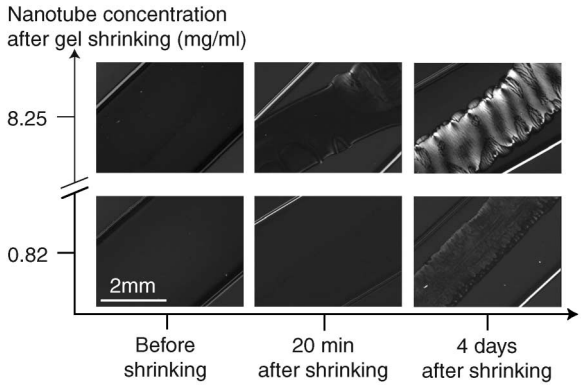

FIG. 2. A summary of the effects of time and concentration on the alignment of nanotubes in NIPA gels.

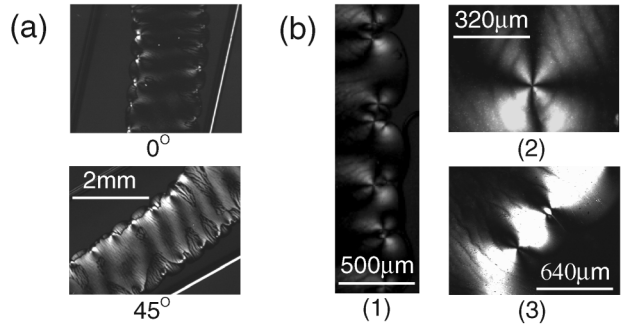

FIG. 3. (a) Birefringence images of a nematic nanotube gel in different orientations with respect to the input polarizer pass axis. (b) Liquid crystalline defects [15] observed near the sample edges. (b1) An array of disclinations with strength +1 or 1 was found in the same sample. (b2) An enlarged image of one of the defects shows four lobes. The dark lines within the bright lobes arise from cracks in the shrunken gel. (b3) In the same sample but at a different location we observe defects with two bright lobes, most likely strength 1/2 disclinations.

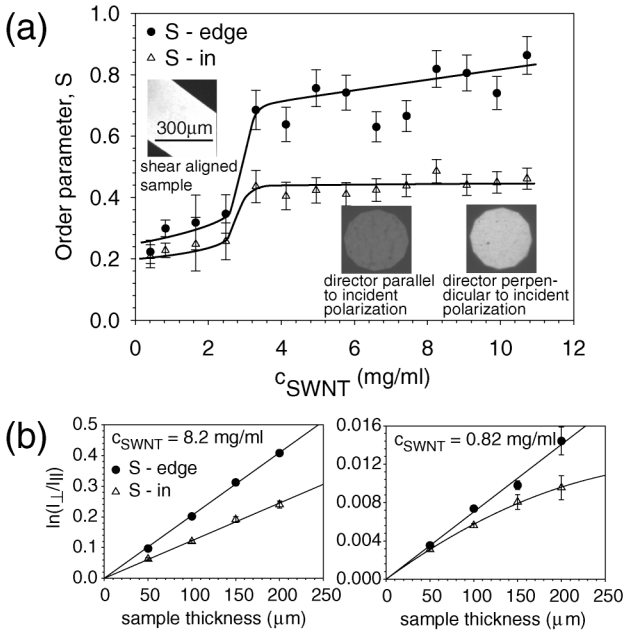

FIG. 4. (a) Order parameter (S) plotted against nanotube concentration in the shrunken SWNT-NIPA gels (c_{SWNT}). Error bars were derived from birefringent domains in multiple samples, and from uncertainty in our estimates of N and L. The inset shows typical images in transmission obtained at the center of the sample for a SWNT-NIPA gel with nanotube concentration 8.25 mg/ml. The illuminated cross section for these measurements was 128 m in diameter, and the illumination wavelength was 647 5 nm. Position-dependent absorption measurements did not detect tube concentration gradients on the 50–100 m scale. $I_{\parallel}$ and $I_{\perp}$ were derived from the average pixel value of each image. Note, if the order parameter of our shear aligned samples were less than unity (as assumed), then the curves would shift vertically and uniformly to lower values, but shapes of these curves and hence the crossover would remain. (b) Light extinction at the edge and the center of gel for c_{SWNT} 8.25 mg/ml showed an exponential decay, whereas for c_{SWNT} 0.82 mg/ml, the extinction was exponential only near the edge. This led us to believe that the nanotube alignment in gels with low nanotube concentration is surface induced.

dark regions became light and the light regions became dark. This is consistent with bulk nanotube alignment parallel to the undulating top and bottom surfaces and the sidewalls. Liquid crystalline defects [Fig. 3(b)] were observed near the sample edges and were most clearly visible in vertical (0) and horizontal (90) orientations. Defects were observed only in samples whose surfaces had developed cusps (i.e., samples with $c_{\mathrm{SWNT}} \geq$ 8.25 mg/ml) and then only near the sample edges. Clearly the shape of the cusps in the buckled regions of the sample play an important role in aligning the director and in creating the geometry required for defects. Observation of these defects strongly supports our view that the SWNTs form a nematic gel phase.

We determined the order parameter of the four-day-old SWNT-NIPA gels as a function of nanotube concentration, gel thickness, and position within the sample. Gel thickness was varied from 50–200 m by using four different rectangular capillaries. We measured the transmission intensities, $I_{\parallel}$ and $I_{\perp}$, of plane polarized light through birefringent domains with polarization, respectively, parallel and perpendicular to the nanotube alignment axis. The inset of Fig. 4(a) shows a pair of such illumination images for a sample with c_{SWNT} 8.25 mg/ml. Light extinction was much larger when the light polarization was oriented parallel to the director. The ratio $I_{\parallel}/I_{\perp}$ differs from unity due to the sample dichroism; it depends on the nanotube nematic order parameter, S, the SWNT number density, N, the sample thickness, L, and the difference, , between the extinction cross sections for tubes oriented parallel and perpendicular to the light polarization direction: $\ln I_{\parallel}/I_{\perp}$ NLS . In our measurements N and L are always known. We measured (9 10^{14} cm^2) using a shear aligned sample for which we assumed S to be 1 [16]. With these assumptions we were able to deduce S as a function of SWNT concentration, position within the sample, and sample thickness. Order parameter variations for domains near the sample edge and center (i.e., ~1 mm from the edge) are exhibited in Fig. 4(a).

Our quantitative observations have several noteworthy features: (i) There is clearly an abrupt increase in both surface and bulk order parameters at c_{SWNT} $c_{\mathrm{crit}} \sim 3.30$ mg/ml. (ii) Samples exhibit weak order ($S \sim 0.2$) at concentrations lower than c_{crit}, which does not fall to zero at the lowest concentrations observed. (iii) Concentrated samples were more substantially aligned. The order parameter in concentrated gels reached ~0.8 near the sample edge, and ~0.4 near the sample center. (iv) Orientational order near the sample center saturates at higher concentrations at values well below unity. Orientational order near sample surfaces exhibits a

very small but noticeable increase with concentration and always remains significantly less than unity.

We propose a simple semimicroscopic model to interpret our observations. We note first that the gel volume shrinks by a factor of 8 or more to produce isolated nanotube concentrations higher than can be sustained in free suspensions without significant nanotube bundling. From this we conclude the gel prevents the close contact between parallel rods that leads to aggregation. From the observed increase in nematic order with time after compression, we conclude rods can move slowly in the gel matrix. Since the maximum nematic order parameter in the bulk is only of order 0.4, much less than the value of 0.84 predicted by Onsager for hard rods at the I-N transition [10], we conclude the gel matrix and possible attractive interactions between the rods severely limit the rotational phase space available to the rods. Since nematic order aligns parallel to the largest sample boundary, and since nematic order is consistently higher at the boundaries than in the bulk, we conclude that sample boundaries provide a surface aligning field.

Figure 4(a) shows an abrupt jump in both surface and bulk order parameters at c_{SWNT} c_{crit}. We interpret this to be the result of a first-order isotropic-to-nematic transition in the bulk. Thus for $c < c_{\mathrm{crit}}$, the order parameter decays exponentially with distance from the sample walls with a profile close to a hyperbolic tangent along straight paths from the top to the bottom of the sample near the center of the largest wall. The slight downward curvature with increasing thickness in $\ln I_{\perp}/I_{\parallel}$ in the center of the c_{SWNT} 0.82 mg/ml sample shown in Fig. 4(b) is consistent with such a profile. The order near the edges of the sample is nearly uniform and $\ln I_{\perp}/I_{\parallel}$ is linear. In the 8.2 mg/ml sample, in which both the surface and the bulk are ordered, $\ln I_{\perp}/I_{\parallel}$ is essentially linear both at the sample center and at the sample edges. Thermotropic nematic elastomers are known [17,18] to stretch in the direction of nematic order. This phenomenon provides us with an explanation of the surface buckling. Since the surface order parameter is greater than that of the bulk for $c > c_{\mathrm{crit}}$, the surface should stretch more than the bulk in the nematic phase. This differential stretch causes the surface to undulate relative to the bulk to increase its overall area. Surface buckling becomes visible after the bulk orders and a large difference between surface and bulk order develops. Buckling becomes more pronounced as this difference increases. This is reminiscent of observations made by others, but in a very different context [19].

In summary, we have made nematic nanotube gels, i.e., gels containing large domains of isolated and oriented single-wall carbon nanotubes. The lyotropic gels represent a new physical system different from both lyotropic hard-rod suspensions and thermotropic elastomers, with which they share the property of nematic order in a randomly cross-linked gel. They may be useful as precursors to create aligned composites. The general mechanism discussed here for inducing lyotropic phase transitions (as opposed to simply increasing concentration [20]) by volume compression of gels may be readily adapted to other complex fluid systems such as colloids and emulsions.

We thank R. Kamien and A.W.C. Lau for useful discussions. This work has been partially supported by the NSF through MRSEC Grants No. DMR 00-79909 and No. DMR-0203378 and by NASA Grant No. NAG8-2172.

[1] T.W. Odom *et al.*, Nature (London) **391**, 62 (1998).
[2] M. J. O'Connell *et al.*, Science **297**, 593 (2002).
[3] S. Fan *et al.*, Science **283**, 512 (1999).
[4] J. Kong *et al.*, Science **287**, 622 (2000).
[5] B. Vigolo *et al.*, Science **290**, 1331 (2000).
[6] R. Haggenmueller *et al.*, Chem. Phys. Lett. **330**, 219 (2000).
[7] V.G. Hadjiev *et al.*, Appl. Phys. Lett. **78**, 3193 (2001).
[8] M. J. O'Connell *et al.*, Chem. Phys. Lett. **342**, 265 (2001).
[9] M. F. Islam *et al.*, Nano Lett. **3**, 269 (2003).
[10] L. Onsager, Ann. N.Y. Acad. Sci. **51**, 627 (1949).
[11] For hard rods of length L and diameter D Onsager predicts an I-N transition at rod volume fraction of ϕ_c 4.2 D_{eff}/L D/D_{eff} ^{2} with D_{eff} $D +$, where represents the increase in effective diameter arising from surfactant coating and electrostatic screening. A 2-nm-thick surfactant layer and a 14-nm charge-screening contribution to at 20 mM buffer increases D_{eff} to 19.35 nm and reduces the critical concentration to 1.1 mg/ml. Mass per unit length for individual nanotubes is 5 10 ^{21} g/nm.
[12] Nanotube suspensions of concentration 1.5 mg/ml contain ~50% isolated SWNTs and the rest small bundles.
[13] F. Ilmain *et al.*, Nature (London) **351**, 400 (1991).
[14] A.G. Rinzler *et al.*, Appl. Phys. A **67**, 29 (1998).
[15] P.M. Chaikin and T.C. Lubensky, *Principles of Condensed Matter Physics* (Cambridge University Press, Cambridge, 1997), 2nd ed.
[16] Shear aligned samples [Fig. 4(a) inset] were prepared by stretching a collapsed SWNT-NIPA gel with c_{SWNT} 8.25 mg/ml along its long axis. The nanotubes aligned along the stretching direction and the gel became extremely birefringent.
[17] G.C. Verwey *et al.*, J. Phys. II (France) **6**, 1273 (1996); H. Finkelmann *et al.*, J. Phys. II (France) **7**, 1059 (1997); M. Warner and E. M. Terentjev, *Liquid Crystal Elastomer* (Oxford University Press, Oxford, 2003).
[18] J.V. Selinger *et al.*, Phys. Rev. Lett. **89**, 225701 (2002).
[19] E. Cerda and L. Mahadevan, Phys. Rev. Lett. **90**, 074302 (2003).
[20] J. M. Weissman *et al.*, Science **274**, 959 (1996).